

Comparative analysis and experimental results of advanced control strategies for vibration suppression in aircraft wings

Isabela R. Birs¹, Silviu Folea¹, Dana Copot², Ovidiu Prodan³, Cristina-I. Muresan¹

¹Department of Automation, Technical University of Cluj-Napoca, Memorandumului St., No. 28, Cluj-Napoca, Romania

²Department of Electrical energy, Systems and Automation, Research group on Dynamical Systems and Control, Ghent University, Technologiepark 914, 2nd floor, 9052 Ghent, Belgium

³Department of Civil Engineering, Technical University of Cluj-Napoca, Memorandumului St., No. 28, Cluj-Napoca, Romania

Cristina.Muresan@aut.utcluj.ro

Abstract. The smart beam is widely used as a means of studying the dynamics and active vibration suppression possibilities in aircraft wings. The advantages obtained through this approach are numerous, among them being aircraft stability and manoeuvrability, turbulence immunity, passenger safety and reduced fatigue damage. The paper presents the tuning of two controllers: Linear Quadratic Regulator and Fractional Order Proportional Derivative controller. The active vibration control methods were tested on a smart beam, vibrations being mitigated through piezoelectric patches. The obtained experimental results are compared in terms of settling time and control effort, experimentally proving that both types of controllers can be successfully used to reduce oscillations. The analysis in this paper provides for a necessary premise regarding the tuning of a fractional order enhanced Linear Quadratic Regulator, by combining the advantages of both control strategies.

1. Introduction

The cantilever wing is the only type of airplane wing used in civilian aircrafts. Due to its shape and the need to actively control vibration, the cantilever wing is characterized and modelled as a smart beam [1]. The active vibration control is most often realized through smart materials exhibiting the piezoelectric effect. The piezo patches, which act as sensors and actuators, are embedded or mounted on the surface of the beam [2], [3].



Among the years, various control strategies have been tested with the purpose of significantly reducing the smart beam's displacement. Such strategies include: fuzzy logic [4], adaptive [5], robust, Linear Quadratic Regulator, fractional – order PI, PD and PID type controllers [6], etc. In [7] the authors present the tuning of a fuzzy logic controller using the particle swarm optimization approach that deals with the control of smart composite beams vibration. The proposed controller is compared with fuzzy logic controllers with constant scaling factors and with the Linear Quadratic Regulator (LQR). The results obtained show that the PSO tuned fuzzy logic controller obtains better vibration suppression when compared to the LQR for both single and multimodal cases. Numerical optimization consisting of population based Particle Swarm Optimization and Genetic Algorithms is also used in [8] to develop fuzzy logic controllers. The study compares the behaviors of the classical fuzzy controller with the ones obtained from the optimization techniques. The controller optimized by PSO yielded better results than the others.

The active control of flexible cantilever plates based on the piezoelectric effect is realized in [9] through artificial neural networks. The neuro-controller is trained such that optimal voltage is applied to the piezoelectric patches. The performance and the robustness of the trained controller is evaluated comparing the active response to the free vibration under various types of dynamic excitations.

The idea of tuning a controller with neural networks is also present in [10] where the parameters of a proportional – derivative controller are determined with a back propagation neural network (BPNN). Data obtained from both simulations and practical experiments is used to prove the veracity of the proposed method. The controller proves to exert vibration on an experimental unit consisting on a vertical aluminum beam equipped with 3 piezoelectric patches. Modeling and controlling smart beams with the hysteresis property is described in [11]. A time varying model of the smart beam is determined based on the hysteresis property using recursive extended least square method. The vibration is controlled with an adaptive minimal variance self-tuning direct regulator (MSVTDR). The advantage of this type of controller consists in computing an optimal control signal. The adaptive regulator claims to reduce the strain of the smart beam with up to 83.67% at its first natural frequency.

Piezoelectric bonded smart structures are controlled with the classical PID controller in [12]. The PID controller is designed to attenuate both free and forced vibrations of the smart beam. Compared with the optimal LQR controller, the PID controller gives the best results. Part of the study is dedicated to analyze the behavior of the three control effects: proportional, derivate and integral. Experimental tests suggest that the D control has little to no effect on the steady-state error, but counteracts the free vibration of the beam. However, the PI effects eliminate the steady state error, but have a negative impact on the free vibration. A feedback control algorithm is implemented in [13] using the real time National Instruments Real Time Controller cRIO 9022 controller. Improvements of 49.29% and 52.84% were obtained for the first and second flexural modes. However, the strain rate feedback approach showed low system stability. The validity of the H_∞ optimal controller is proven in [14] when uncertain disturbance and measurement noise are considered. A full-order state observer LQR and PID controllers are designed and tested in order to control the vibration of the beam [15]. The LQR controller outperformed the integer-order PID in the 3 configurations studied of the beam-piezoelectric elements.

In this study, two active vibration control methods are proposed with the purpose of significantly reducing the settling time of a dedicated smart beam when rejecting disturbances. The first choice regarding the control algorithm refers to a LQR controller, mainly chosen because of its wide application in smart beam vibration suppression methods, the simple parameter design method, as well as overall efficiency. The second control algorithm is a rather less used approach in vibration suppression: the fractional order PD controller, mainly chosen because of its improved performance over classical PID controllers [16]. Apart from that, fractional order systems and controllers are becoming more and more popular in the research community [17], [18]. In terms of vibration suppression in a cantilever beam, fractional order PD controllers have been designed previously for similar cantilever beam and the experimental results demonstrated the advantages of using a fractional order PD controller instead of the classical integer order PD controller [19].

To tune the controllers, the dynamics of the smart beam is considered as a simple second order system. In this way, because of the simplification of the model, the problem of robustness is also addressed, since in real life applications, the ability of the control system to cope with modeling uncertainties proves extremely useful, especially in the case of an aircraft subjected to turbulences of different frequencies. The two proposed methods were implemented and validated on an experimental vibration unit consisting of an aluminum cantilever beam equipped with piezoelectric patches. The comparison is realized by analyzing the settling times and control effort obtained while the beam is subjected to impulse disturbances.

The structure of the article presents an overview of the proposed tuning methods, the description of the experimental stand, experimental system identification, numerical and experimental results and last, but not least, the conclusions.

2. Overview of the proposed active vibration control methods

2.1. Linear Quadratic Regulator (LQR)

The LQR is an optimal controller that ensures the stability of the closed-loop system, has a simple tuning procedure and a certain degree of robustness. This type of optimal controller minimizes a cost function of the following form:

$$J_{LQR} = \int_0^{\infty} [x^T(t) * Q * x(t) + u^T(t) * R * u(t)] dt \quad (1)$$

where R is a scalar and Q is a positive semi-definite matrix (symmetric matrix) having the dimension $n \times n$, with n the number of states of the state space system that describes the dynamics of the smart beam. The state space system is given as:

$$\begin{aligned} \dot{x}(t) &= Ax(t) + Bu(t) \\ y(t) &= Cx(t) + Du(t) \end{aligned} \quad (2)$$

where x is the state vector; y is the output vector; u is the control signal and A is the state matrix, B the control matrix, C the output matrix and D is the feedthrough matrix.

The integral from equation (1) is written as a sum of the accumulated deviation of the states with respect to the equilibrium point and the accumulated control effort. By properly choosing the parameters Q and R , the importance of the control performance and input energy are weighted reaching a convenient compromise.

The manipulated input $u(t)$ generated by the LQR controller is

$$u(t) = -Kx(t) \quad (3)$$

where K is the feedback gain matrix computed as

$$K = R^{-1} \cdot B^T \cdot X \quad (4)$$

X is a symmetric matrix determined from the Ricatti equation as a nonnegative definite solution:

$$A^T X + XA + C^T Q C - XBR^{-1}B^T X = 0 \quad (5)$$

The resulting closed loop system has the form:

$$\dot{x}(t) = (A - B * K) * x(t) \quad (6)$$

2.2. Fractional – order Proportional Derivative Controller

The fractional-order PD controller is best defined by its transfer function:

$$H_{FO-PD}(s) = k_p (1 + k_d s^\mu) \quad (7)$$

where s is the Laplace operator, k_p and k_d are the proportional and derivative gains, while μ is the fractional order differentiator. When μ is equal to 1, equation (7) describes an integer order proportional – derivative controller.

The trigonometric form of the fractional order PD (FO-PD) controller can be written by moving from the Laplace domain to the frequency domain, where $j\omega$ replaces s .

$$H_{FO-PD}(j\omega) = k_p \left[1 + k_d \omega^\mu \left(\cos\left(\frac{\pi\mu}{2}\right) + j \sin\left(\frac{\pi\mu}{2}\right) \right) \right] \quad (8)$$

The three parameters of the controller are computed based on frequency domain constraints: phase margin φ_m , gain crossover frequency ω_{cg} and robustness to gain variations. The first two constraints can be written through the phase equation of the open loop system:

$$\angle(H_{open-loop}(j\omega_{cg})) = -\pi + \varphi_m \quad (9)$$

The gain crossover frequency is mathematically expressed as:

$$|H_{open-loop}(j\omega_{cg})| = 1 \quad (10)$$

The robustness constraint is imposed such that it ensures a constant overshoot at gain variations. On the Bode phase plot, a constant overshoot means a constant phase near the gain crossover frequency. A constant phase graphically translates into a straight line. One important property of a straight line is the fact that its derivative is equal to 0. This means that if the derivative of the phase margin is imposed as being 0 at the gain crossover frequency, the closed loop robustness is assured.

$$\left. \frac{d(\angle H_{open-loop}(\omega))}{d\omega} \right|_{\omega=\omega_{cg}} = 0 \quad (11)$$

The open-loop system, with $G(s)$ – the transfer function of the smart beam and $C(s)$ – that of the FO-PD controller, is computed as:

$$H_{open-loop}(s) = G(s) \cdot C(s) \quad (12)$$

Replacing the equation of the open-loop transfer function in the gain crossover, phase margin and robustness constraints from equations (9),(10) and (11), the modulus, phase and phase derivative of the controller $C(s)$ are obtained in the complex representation:

$$\begin{aligned}
\angle C(j\omega_{cg}) &= -\pi + \phi_m - \angle G(j\omega_{cg}) \\
|C(j\omega_{cg})| &= \frac{1}{|G(j\omega_{cg})|} \\
\frac{d(C(j\omega))}{d\omega} \bigg|_{\omega=\omega_{cg}} + \frac{d(\angle G(j\omega))}{d\omega} \bigg|_{\omega=\omega_{cg}} &= 0
\end{aligned} \tag{13}$$

Further using (8) in the phase equation from (13) leads to:

$$\frac{k_d \omega_{cg}^\mu \sin\left(\frac{\pi\mu}{2}\right)}{1 + k_d \omega_{cg}^\mu \cos\left(\frac{\pi\mu}{2}\right)} = \tan(-\pi + \phi_m - \angle G(j\omega_{cg})) \tag{14}$$

while the robustness constraint may be rewritten as:

$$\frac{\mu k_d \omega_{cg}^{\mu-1} \sin\frac{\pi\mu}{2}}{1 + 2k_d \omega_{cg}^\mu \cos\frac{\pi\mu}{2} + k_d^2 \omega_{cg}^{2\mu}} = - \frac{d(\angle G(j\omega))}{d\omega} \bigg|_{\omega=\omega_{cg}} \tag{15}$$

By solving (14) and (15), as a system of equations, the derivative gain and the fractional order, k_d and μ , are obtained. The graphical method can be a tangible approach to determining the parameters.

Rewriting the magnitude condition from equation (13) such that the proportional gain is isolated in the left side, the following equation is obtained, from which k_p is easily determined:

$$k_p = \frac{1}{|G(j\omega_{cg})|} \frac{1}{\sqrt{1 + 2k_d \omega_{cg}^\mu \cos\frac{\pi\mu}{2} + k_d^2 \omega_{cg}^{2\mu}}} \tag{16}$$

3. Experimental setup and system identification

3.1. Description of the experimental equipment and the smart beam

The experimental vibration unit can be seen in Figure 1 and consists of a smart beam equipped with 4 piezoelectric (PZT) actuators, a real-time controller, input and output modules and a PZT controller. The beam is fixed at one end allowing only back and forth movements. There are four piezoelectric patches mounted close to the fixed end of the beam, two on each side. The aluminium beam is 250 mm long, 20 mm wide and 1 mm thick. Figure 2 shows a detailed view of the smart beam and the position of the patches. Two piezoelectric DuraAct P-878 Power Patch transducers are fixed on each side of the beam.

The control algorithm is implemented in real-time with the help of the CompactRIO™ 9014 controller. The NI 9230 is the input module that measures the displacement of the beam, while the NI 9263 output module is used for applying the voltage to the patches used to mitigate vibration. The communication and the control algorithms are implemented in LabVIEW™.

The piezoelectric patches are used only as actuators and not as sensors because the movement of the beam is measured with the 120 ohm Omega Prewired KFG-5-120-C1-11L1M2R strain gauge sensors. The E-509.X3 module from Physik Instrumente is used to amplify the signal from the sensors, while E-503.00 is used to amplify the control signal to the PZT patches. The chassis amplifies the

signal by 10, meaning that if the LabVIEW code gives a control signal of between $[-2;2]$ volts, the patches are excited with a signal between $[-20; 20]$ volts.

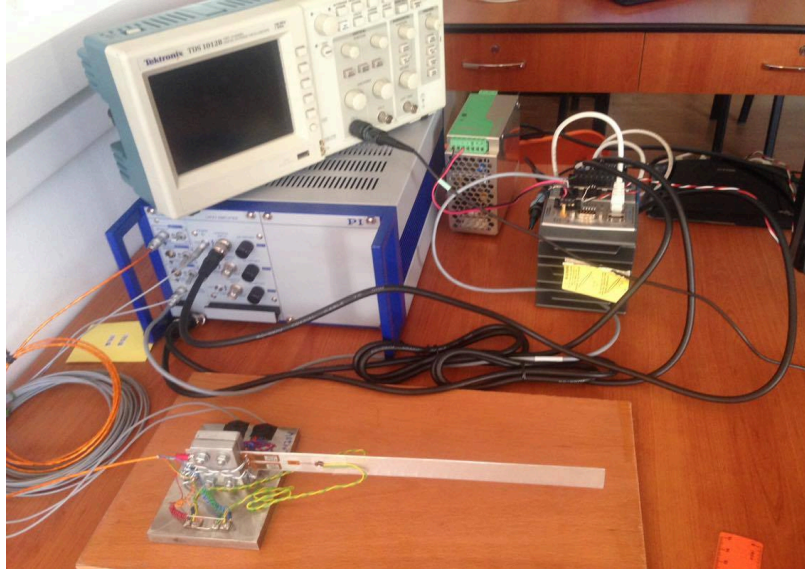


Figure 1. Experimental setup

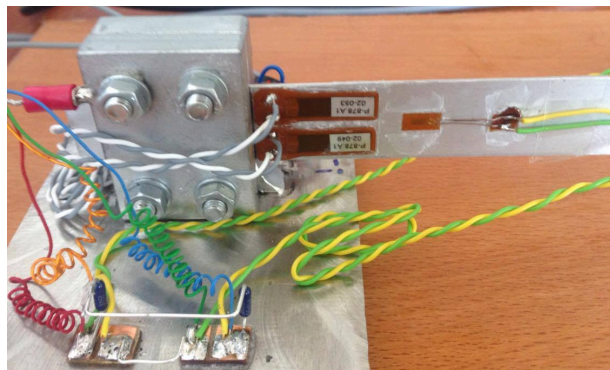


Figure 2. Detailed view of the fixed end of the smart beam.

3.2. System Identification

The transfer function of the system is determined based on the experimental response of the beam to a sinusoidal input. In order to determine an accurate transfer function the system was excited with sine waves of different amplitudes and frequencies.

It was experimentally observed that the resonant frequency of the smart beam is close to 14.52 Hz. A second order model of the smart beam has been determined as:

$$G(s) = \frac{72.99}{s^2 + 1.115s + 8401} \quad (17)$$

The validation of the identified model $G(s)$ to a sine input of frequency 14.52 Hz and amplitude 10 V is shown in Figures 3, 4 and 5 below.

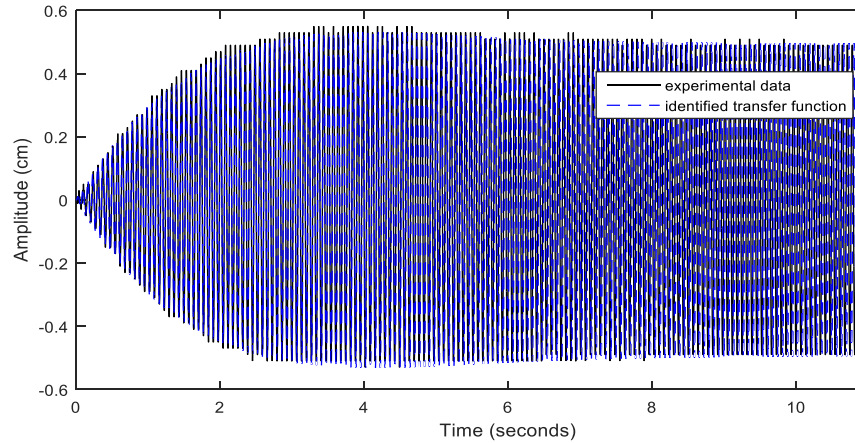


Figure 3. Experimental data and second order simulated response of the second order transfer function

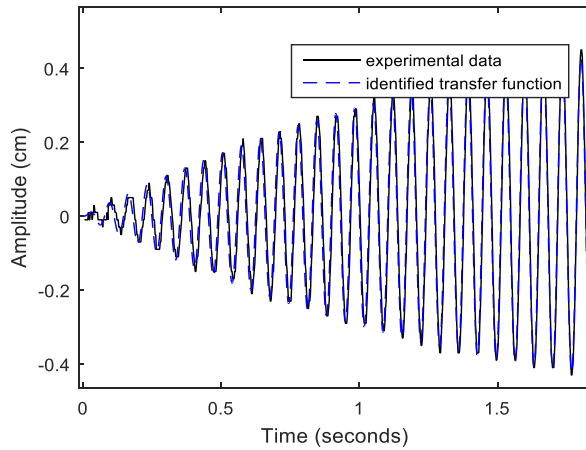


Figure 4. Zoomed transient response fit of the identified second order transfer function

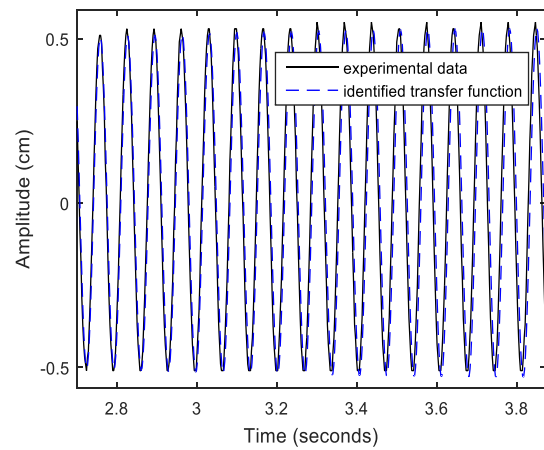


Figure 5. Zoomed steady state response fit of the identified second order transfer function

As can be seen in the figures above, the model fits the experimental data accurately, with a 97.07% fit to estimation data, a FPE (Final Prediction Error) of $9.85031 \cdot 10^{-5}$ and a MSE (Mean Squared Error) equal to $9.829 \cdot 10^{-5}$. The resonant frequency of the model $G(s)$ is 14.59 Hz, resulting in a small modelling error compared to the experimentally observed resonant frequency of 14.52 Hz.

4. Controller tuning and experimental results

4.1. LQR controller tuning

For the LQR controller tuning, the state-space representation of the beam is needed:

$$A = \begin{pmatrix} 0 & 1 \\ -8401 & -1.115 \end{pmatrix} \quad B = \begin{pmatrix} 0 \\ 72.99 \end{pmatrix} \quad (18)$$

$$C = (1 \quad 0) \quad D = (0)$$

where the states of the state space system in (18) are the beam displacement and its velocity.

The weighting matrices R and Q are chosen as follows:

$$Q = \begin{pmatrix} 1 & 0 \\ 0 & 0.002 \end{pmatrix} \quad R = 3 \quad (19)$$

The discrete feedback gain matrix, K , is determined as:

$$K = (-0.1913 \quad 0.0152) \quad (20)$$

where a sampling period of 0.003 seconds has been used. The choice for the Q and R parameters is based on a strict requirement for the control signal to be kept in a range $[-2, 2]$, corresponding to a $[-20, +20]$ V applied on the PZT patches. By trial and error, the best settling time, with the control signal limitation constraint, has been obtained for Q and R as indicated in (19). The LQR controller in (20) was implemented on the experimental unit and the closed loop results can be seen in Figure 6. An impulse disturbance acting on the beam's free end of 0.5V has been considered. The control signal required to reduce the vibrations is given in Figure 7.

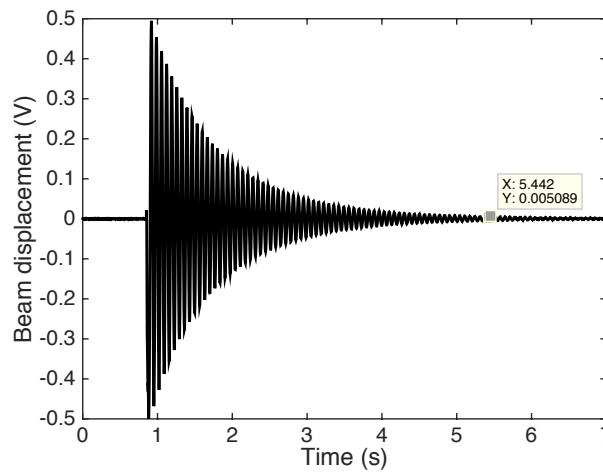


Figure 6. Closed-loop system response using the LQR controller

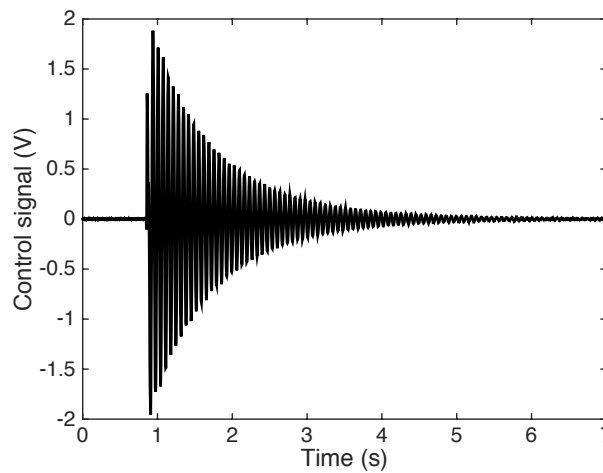


Figure 7. The control signal generated by the LQR controller

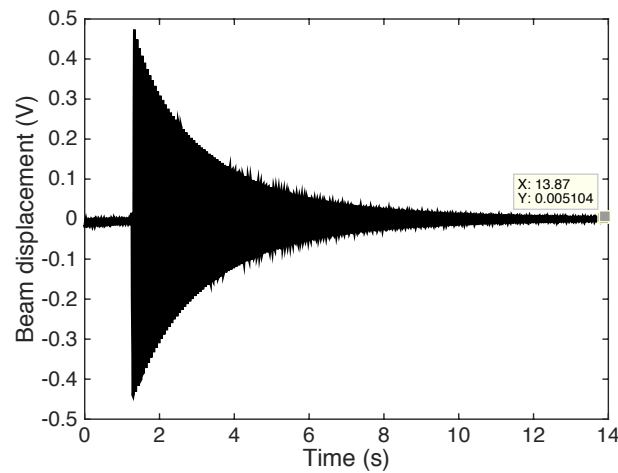


Figure 8. Free vibration of the smart beam considering an impulse disturbance

As can be seen in the figures above, the Linear Quadratic Regulator can be successfully used to suppress unwanted vibrations, the settling time achieved in this case being of 5.44 seconds. Compared to the settling time of 13.87 seconds for the passive free vibration, as indicated in Figure 8, the LQR controller provides for a 60.8% improvement. An important advantage of the LQR controller is that the feedback gain matrix, K , is relatively easy to compute even in the case of a higher order model.

4.2. Fractional – Order Proportional Derivative Controller tuning

The fractional-order PD controller is tuned by imposing frequency domain constraints: a phase margin of 60° for a lower overshoot of the closed loop system, a gain crossover frequency of 105 rad/s for a small settling time and the robustness to gain variations, as indicated in (13).

The obtained fractional-order PD controller, with the parameters computed according to (14), (15) and (16) above is given by :

$$H_{\text{FO-PD}}(s) = 15.36 \left(1 + 0.028 s^{0.9164} \right) \quad (21)$$

The frequency response of the open loop system with the FO-PD controller in (21) demonstrates that the performance criteria are met and it is given in Figure 9. To implement the FO-PD controller in (21), its discrete time approximation has been determined using the new method described in [20], with a sampling period of 0.003 seconds.

The closed loop response of the smart beam, under the same impulse disturbance as in the case of the LQR controller, is given in Figure 10, while the control signal is given in Figure 11. In this case, the FO-PD tuning method has not directly considered the control signal limitation constraint. As indicated in Figure 11, the FO-PD controller has a much more aggressive dynamics in comparison to the LQR controller, as seen in Figure 7. Also, the derivative action of the FO-PD controller is highly sensitive to noise. Nevertheless, this aggressive dynamics leads to better performance in terms of settling time. In the case of the FO-PD controller, the disturbance is rejected entirely in 3.24 seconds, which represents a 76.6% improvement compared to the free vibration and a 40.4% improvement in comparison to the LQR controller.

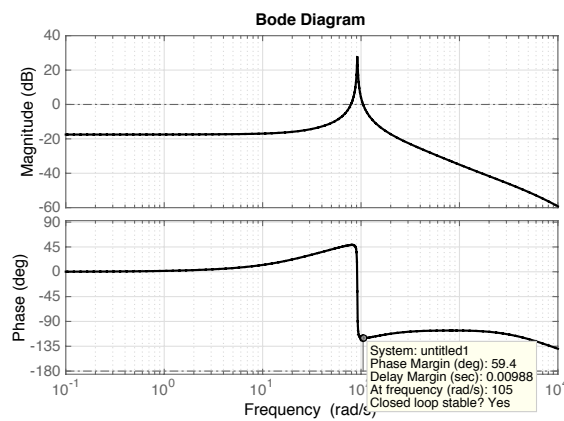


Figure 9. Bode diagram of the open loop system with FO-PD controller

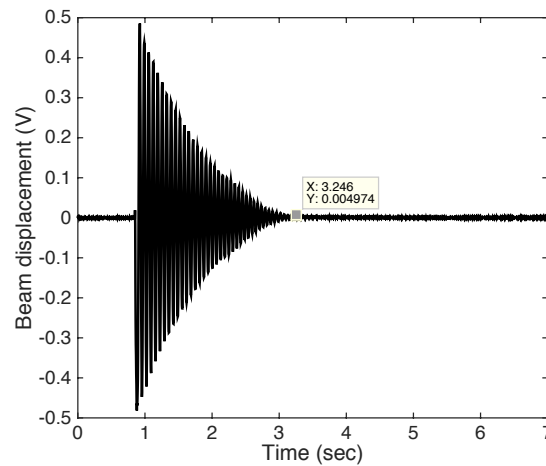


Figure 10. The closed-loop system response using a FO-PD controller

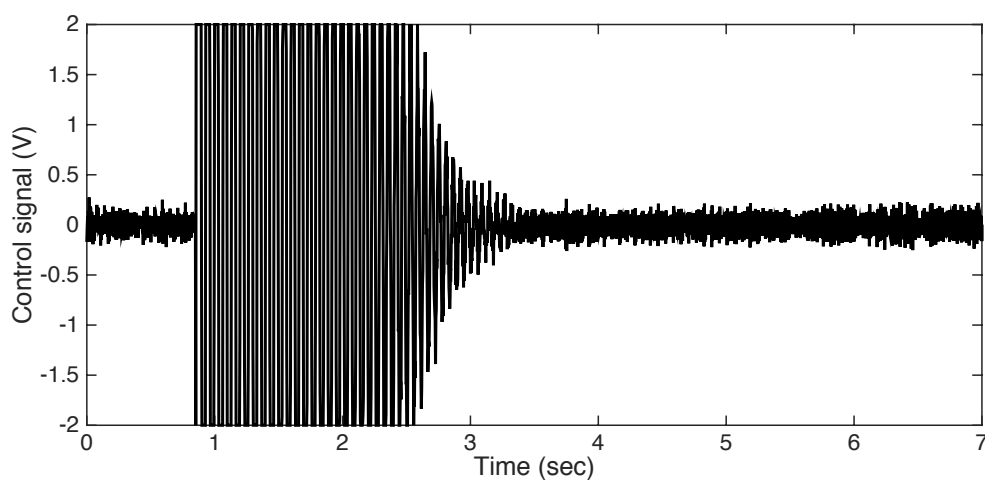


Figure 11. The control signal generated by the FO-PD controller

5. Conclusions

From the settling time point of view, the fractional-order PD controller brings a significant improvement compared to the LQR controller, as has been pointed out in this paper. However, the nearly 50% improvement in the settling time comes with a disadvantages regarding the increase in the control effort. These preliminary results of the FO-PD controller in suppressing vibrations on a smart beam through piezoelectric patches are a novel application study and further research and improvement will be sought. A major focus will be given to the design of a fractional order PID controller that considers directly in the tuning procedure the limitations on the control signal, to avoid the saturation. Also, since the LQR controller provides for an acceptable vibration attenuation, this too can be further enhance by combining its benefits with that of fractional calculus, in tuning a fractional order LQR controller. The analysis in this paper constitutes an important premise in that regard.

References

- [1] Dr. Hatem, R. Wasmi Hussein Abdulridha Abdulameer, "Vibration Control Analysis of Aircraft Wing by Using Smart Material," *Innovative Systems Design and Engineering*, vol. 6, no. 8, 2015.
- [2] Ahmed Abdul-hussain Ali, Hussain Yousif Mahmood, and Mahmood Wael Saeed, "Active Vibration Control of Aircraft Wing Using Piezoelectric Transducers," *International Journal of Scientific & Engineering Research*, vol. 7, no. 5, May 2016.
- [3] Shashikala Prakash et al., "Active vibration control of a full scale aircraft wing using a reconfigurable controller," *Journal of Sound and Vibration*, vol. 361, pp. 32-49, January 2016.
- [4] Mohammad A. Ayoubi, Sean Shan-Min Swei, and Nhan T. Nguyen, "Fuzzy model-based pitch stabilization and wing vibration suppression of flexible aircraft," in *2014 American Control Conference*, Portland, OR, 4-6 June 2014, pp. 3083 - 3088.
- [5] Gergely Takács, Tomáš Polóni, and Boris Rohal'-Ilkiv, "Adaptive Model Predictive Vibration Control of a Cantilever Beam with Real-Time Parameter Estimation," *Shock and Vibration*, 2014.
- [6] Muresan Cristina, Folea Silviu, Prodan Ovidiu, and Eva Dulf, "Design and Experimental Validation of an Optimal Fractional Order Controller for Vibration Suppression," in *The International Conference on Control, Decision and Information Technologies*, Malta, April 6-8, 2016.
- [7] Nemanja D. Zorić et al., "Free vibration control of smart composite beams using swarm optimized self-tuning fuzzy logic controller," *Journal of Sound and Vibration*, vol. 333, no. 21, pp. 5244-5268, October 2014.
- [8] Magdalene Marinaki, Yannis Marinakis, and Georgios E. Stavroulakis, "Fuzzy control optimized by PSO for vibration suppression of beams," *Control Engineering Practice*, vol. 18, no. 6, pp. 618-629, June 2010.
- [9] Osama Abdeljaber, Onur Avci, and Daniel J. Inman, "Active vibration control of flexible cantilever plates using piezoelectric materials and artificial neural networks," *Journal of Sound and Vibration*, vol. 363, pp. 33-53, February 2016.
- [10] Zhicheng Qiu, Xiangtong Zhang, and Chunde Ye, "Vibration suppression of a flexible piezoelectric beam using BP neural network controller," *Acta Mechanica Solida Sinica*, vol. 25, no. 4, pp. 417-428, August 2012.
- [11] Ting Zhang, Hong Guang Li, and Guo Ping Cai, "Hysteresis identification and adaptive vibration control for a smart cantilever beam by a piezoelectric actuator," *Sensors and Actuators A: Physical*, vol. 203, pp. 168-175, December 2013.
- [12] Shunqi Zhang, Rüdiger Schmidt, and Xiansheng Qin, "Active vibration control of piezoelectric

- bonded smart structures using PID algorithm," Chinese Journal of Aeronautics, vol. 28, no. 1, pp. 305-313, February 2015. [Online]. <http://dx.doi.org/10.1016/j.cja.2014.12.005>
- [13] Riessom Weldegiorgis, Prasad Krishna, and K.V. Gangadharan, "Vibration Control of Smart Cantilever Beam Using Strain Rate Feedback," in International Conference on Advances in Manufacturing and Materials Engineering, ICAMME, 2014, pp. 113-122.
 - [14] Hu Junfeng, Zhu Dachang, and Chen Qiang, "Vibration Control of a Smart Beam Using H^∞ Control," in Fourth International Conference on Intelligent Computation Technology and Automation, 2011.
 - [15] Harijono Djojodihardjo, Mohammad Jafari, Surjatin Wiriadidjaja, and Kamarul Arifin Ahmad, "Active Vibration Suppression of an elastic piezoelectric sensor and actuator fitted cantilevered beam configurations as a generic smart composite structure," Composite Structures, vol. 132, pp. 848-863, August 2015.
 - [16] C.A. Monje, YangQuan Chen, Blas M. Vinagre, D. Xue, Vicente Feliu, Fractional order Systems and Controls: Fundamentals and Applications, Springer-Verlag, London, 2010
 - [17] Robin De Keyser, Cristina I. Muresan, Clara M. Ionescu, A novel auto-tuning method for fractional order PI/PD controllers, ISA Transactions, vol. 62, pp. 268-275, May 2016
 - [18] Clara M. Ionescu, Jose A. Tenreiro Machado, Robin De Keyser, Fractional-order impulse response of the respiratory system, Computers & Mathematics with Applications, vol. 62, no. 3, pp. 845-854, August 2011
 - [19] Birs, I.R., Muresan, C.I., Folea, S., Prodan, O. (2016), A Comparison between Integer and Fractional Order PD_μ Controllers for Vibration Suppression, *Applied Mathematics and Nonlinear Sciences*, Vol. 1, No. 1, pp. 273-282, DOI:10.21042/AMNS.2016.1.00022
 - [20] Robin De Keyser, Cristina Muresan, and Clara Ionescu, "A low-order computationally efficient approximation of fractional order systems," Automatica (under review), 2016